THE JOURNAL OF BIOLOGICAL CHEMISTRY
Vol. 278, No. 40, Issue of October 3, pp. 38247–38253, 2003

Printed in U.S.A.

Antifolding Activity of the SecB Chaperone Is Essential for Secretion of HasA, a Quickly Folding ABC Pathway Substrate*[S]

Received for publication, March 6, 2003, and in revised form, June 26, 2003
Published, JBC Papers in Press, June 26, 2003, DOI 10.1074/jbc.M302322200

Nicolas Wolff‡, Guillaume Sapriel§, Christophe Bodenreider¶, Alain Chaffotte¶, and Philippe Delepelaire§‖

From the ‡Unité de Résonance Magnétique Nucléaire des Biomolécules, the ¶Unité de Repliement et Modélisation des Protéines, and the §Unité des Membranes Bactériennes CNRS UMR2172, Institut Pasteur, 25–28 rue du Dr. Roux, 75724 Paris Cedex 15, France

We have previously shown that SecB, the ATP-independent chaperone of the Sec pathway, is required for the secretion of the HasA hemophore from *Serratia marcescens* via its type I secretion pathway, both in the reconstituted system in *Escherichia coli* and in the original host. The refolding of apo-HasA after denaturation with guanidine HCl was followed by stopped-flow measurements of fluorescence of its single tryptophan, both in the absence and presence of SecB. In the absence of SecB, HasA folds very quickly with one main phase (45 s^{-1}) accounting for 92% of the signal. SecB considerably slows down HasA folding. At stoichiometric amounts of SecB and HasA, a single phase (0.014 s^{-1}) of refolding is observed. Two double point mutants of HasA were made, abolishing two hydrogen bonds between N-terminal and C-terminal side chain residues. In both cases, the mutants essentially maintained the same secondary and tertiary structure as wild-type HasA and were fully functional. Refolding of both mutants was much slower than that of wild-type HasA and they were secreted essentially independently of SecB. We conclude that SecB has mainly an antifolding function in the HasA ABC secretion pathway.

SecB is a chaperone of the Sec pathway in Gram-negative bacteria. It was initially identified in *Escherichia coli* where it interacts with a subset of preproteins to be exported across the cytoplasmic membrane in such a way as to slow down their folding and target them to SecA, the ATPase of the Sec system (1–4) (5). Currently, this chaperone is restricted to Gram-negative bacteria, from the proteobacteria class.

In the Sec pathway, the basis of the interaction of SecB with its substrates has been studied in great detail either *in vivo* for its natural substrates or *in vitro* with its natural or artificial substrates. It appears that *in vitro*, SecB is able to interact with a large variety of denatured substrates whereas it is highly specific *in vivo* (6, 7).

The structure of SecB from *Haemophilus influenzae* is known at atomic resolution and has highlighted several important features of this chaperone (8). It is a tetramer composed of a dimer of dimers. Each monomer bears a putative peptide-binding site able to accommodate, in an extended conformation, hydrophobic peptides of 10–15 residues; on both sides the tetramer presents a patch of negatively charged residues that can interact with a SecA dimer. *In vitro* studies using peptide libraries have indicated that SecB binding site is around 9–10 residues long with a strong preference for aromatic and cationic amino acid residues (9). Furthermore, SecB is a highly negatively charged molecule; thus, negatively charged peptides bind to SecB only if the peptide contains enough aromatic residues in the peptide to overcome the electrostatic repulsion.

Maltose-binding protein (MBP),[1] the best characterized SecB substrate in both *in vivo* and *in vitro* studies, interacts with SecB in kinetic partitioning: the competition between binding to the chaperone and folding reactions (10–13). At 25 °C MBP refolds by a complex pathway characterized by three phases. SecB slows down folding but does not block it; moreover, increasing amounts of SecB progressively slow down MBP refolding. At 5 °C MBP refolding is slower and SecB totally blocks refolding. This can be visualized by the existence of stable SecB·MBP complexes that can be isolated at 5 °C but not at 25 °C. MBP mutants have been isolated on the basis of their ability to translocate across the inner membrane without the presence of SecB. MBPY283D is a MBP mutant that is perfectly biologically active and folds more slowly than wild-type MBP making its translocation SecB-independent (2, 14). This variant associates with SecB blocking MBP folding even at 25 °C. A model has been proposed for the interaction of SecB and MBP: an unfolded form of MBP binds to SecB and is in equilibrium with unbound form. MBP does not fold on SecB and this explains the progressive blockade of MBP folding with increasing SecB amounts. Although the signal sequence of pre-LamB or pre-MBP does not interact with SecB by itself, it slows down the folding of the mature part of the protein (15, 16). SecB interacts with several parts of precursor molecules, protecting a large central portion of precursors to which it is bound (17–19).

Other substrates have been studied in great detail, like barnase of *Bacillus amyloliquefaciens* (20) or R-BPTI (21). Studies with R-BPTI, which is a stable unfolded form of BPTI, have shown that association of a substrate with SecB is limited by diffusion and that the bound R-BPTI is easily exchanged with free R-BPTI. Such findings allowed the researchers to estimate a K_d of a few nM for the SecB·R-BPTI complex. In the case of barnase, which is a small secreted RNase with a standard signal peptide, SecB retards the folding of barnase but never blocks its folding in contrast to what has been observed with MBP. Barnase folds at least partially onto SecB which challenges the kinetics partition model.

* The costs of publication of this article were defrayed in part by the payment of page charges. This article must therefore be hereby marked "*advertisement*" in accordance with 18 U.S.C. Section 1734 solely to indicate this fact.

[S] The on-line version of this article (available at http://www.jbc.org) contains a supplemental figure.

‖ To whom correspondence should be addressed. Tel.: 33-1-40-61-32-76; Fax: 33-1-45-68-87-90; E-mail: pdelep@pasteur.fr.

[1] The abbreviations used are: MBP, maltose-binding protein; GdnHCl, guanidine HCl; WT, wild-type.

We have shown that, besides its function in the Sec pathway, SecB is also the chaperone of a sec-independent pathway, namely the secretion of the $HasA_{SM}$ hemophore through its ABC pathway in *Serratia marcescens* (22, 23).

$HasA_{SM}$ is a monomeric protein of 188 residues secreted by an ABC-type pathway under iron starvation conditions by *S. marcescens* (24) and other Gram-negative bacteria, *Pseudomonas aeruginosa*, *Pseudomonas fluorescens*, and *Yersinia pestis* (25, 26). $HasA_{SM}$ acquires the heme from hemoproteins (*e.g.* hemoglobin) and delivers it to a specific receptor at the cell surface whereby the heme is internalized and used as an iron source (27). Both the secretion pathways and the heme acquisition pathways have been reconstituted in *E. coli*. We have shown that SecB, the chaperone of the Sec pathway, is required for $HasA_{SM}$ secretion both in the original host and in the reconstituted system (22, 23). SecB does not affect the secretion apparatus but likely interacts with $HasA_{SM}$. We have proposed that the N-terminal part of $HasA_{SM}$ interacts in a SecB-dependent fashion with the ABC transporter (28). Folded $HasA_{SM}$ is not secretion-competent and inhibits further secretion of newly synthesized $HasA_{SM}$. This strongly supports a model whereby $HasA_{SM}$ is targeted in a cotranslational fashion to the ABC transporter before secretion via the C-terminal secretion signal (29). Altogether, these data are consistent with a model whereby both the N terminus and the C terminus of $HasA_{SM}$ play a role in secretion.

Here we studied the *in vitro* refolding of $HasA_{SM}$ both in the presence and absence of SecB. We show that HasA protein folds very quickly. Also, we show that SecB interacts directly and quickly with $HasA_{SM}$ to slow down $HasA_{SM}$ folding. We had previously established that the N terminus of HasA also plays a role in secretion. Here we provide evidence that hydrogen bonds which exist between N-terminal and C-terminal residues of $HasA_{SM}$ are involved in $HasA_{SM}$ folding and its SecB dependence for secretion.

EXPERIMENTAL PROCEDURES

Plasmids, Strains, and Growth Conditions—Strains were usually grown at 30 °C in LB medium or M9 minimal medium with 0.4% glycerol as the carbon source. MC4100 and MC4100Δ*secB* were from the lab collection and PAP105 was used for cloning. The following sets of oligonucleotides were used for *in vitro* mutagenesis of *hasA*: ggcattttcagtcaatgcggacagcagcttcggcg (7A+) and cgccgaagctgctgtccgcattgactgaaaatgcc (7A−), cggcggttacagcattgcggactatctgggccagt (17A+) and actggccagatagtccgcaatgctgtaaccgccg (17A−), cgataccggcgcgctggcgaccgcgctgaacggca (148A+) and tgccgttcagcgcggtcgccagcgcgccggtatcg (148A−), and cgtcaactccaccttcgcgcaggtggcggcggcga (167A+) tcgccgccgccacctgcgcgaaggtggagttgacg (167A−).

pSYC134/pUC was used as a template and the quick-change kit from Stratagene used for mutagenesis. Two successive rounds of mutagenesis were carried out to obtain the double mutants. Sequencing was used to verify the mutations. The mutated fragments were then reintroduced into pAM238 and pBGS18+. pSYC150 encodes HasD and HasE, which, together with chromosomally encoded TolC, formed the secretion apparatus. PsecB/trc was used to overproduce SecB. This plasmid contains the *secB* gene under the control of ptrc and was kindly provided by Dr. J. M. Betton.

Materials—GdnHCl ultrapure was from ICN Biomedicals. Cells used for fluorescence and circular dichroïsm were from Hellma.

Expression and Purification of the $HasA_{SM}$ Proteins—Wild-type $HasA_{SM}$ was produced in *E. coli* MC4100(pSYC134/pAM238 + pSYC150) (24). Mutant *hasA* genes were constructed by *in vitro* site-directed mutagenesis. Wild-type (WT), E148A,D167A, and H32A,Y75A mutant samples were produced in M9 minimal medium as reported previously (30) Y7A/H17A mutant was produced in M9 minimal medium with addition of 0.2% bactotryptone. Wild-type and mutant apo-$HasA_{SM}$ proteins were purified as described previously (30). Their heme content, determined by the absorbance of the Soret band wavelength, was always less than 5%. SecB was purified according to published protocol (9). Its purity was checked by SDS-PAGE and the concentration determined from absorbance at 277 nm using an extinction coefficient of 11708 M^{-1} cm^{-1} for the monomer.

To assess the secretion of wild-type and mutant HasA proteins, cultures of MC4100 or MC4100Δ*secB* harboring Has secretion functions from pSYC150 and wild-type or mutant *hasA* on a compatible plasmid were grown in LB medium at 30 °C with the appropriate antibiotics to late exponential phase. The culture was centrifuged at $4000 \times g_{max}$ for 10 min and the supernatant precipitated with 20% trichloroacetic acid was analyzed by SDS-PAGE.

Buffer—All kinetic and equilibrium experiments were carried out in 20 mM sodium phosphate, pH 7.0. The protein concentrations were determined by absorbance spectrophotometry before use. Water was deionized and purified on a Millipore system. All solutions were filtered. The equilibrium unfolding as a function of GdnHCl concentration were carried out by dilution of the proper amount of the 8 M denaturant stock solution and leaving the samples at room temperature overnight prior to performing the titration experiments.

Equilibrium Unfolding Experiments—The equilibrium unfolding of $HasA_{SM}$ and its mutants as a function of GdnHCl concentration was monitored by fluorescence and far-UV CD at 25 °C. Fluoromax (Spex Industries) photon counting spectrophotometer was used carry out the fluorescence studies. The samples were excited at 295 nm, and the resulting emission spectra were acquired between 310 nm and 410 nm. When working at a constant emission wavelength (*i.e.* the protein was excited at 295 nm and emission was monitored at 360 nm), fluorescence intensity was recorded for 30 s, with a sampling period and an integration time of 1 s, and then averaged. The slit width was 5 nm for the excitation light and 10 nm for the emission light. Measurements were made with a protein concentration of 3 μM and a 1.0-cm path length cuvette.

CD measurements were acquired in a Jobin-Yvon CD6 spectropolarimeter. Far-UV CD spectra were obtained by averaging five individual scans with a constant 0.5 nm step and with 5-s integration time from 180 to 200 nm and 2 s from 200 to 260 nm. A cell with a path length of 0.2 cm was used with a protein concentration of 3 μM. Near-UV CD spectra were acquired between 350 nm and 450 nm using 30 μM of protein in a 1.0-cm path length cell. For GdnHCl titrations, the absorbances were measured at 222 nm with a sampling period and time constant of 1 s during 60 s. The final ellipticity was calculated by averaging the 60 recorded values. Measurements were made with a protein concentration of 30 μM in a 0.02-cm path length cell. All spectra were corrected by subtracting the appropriate baseline.

Thermal Denaturation—Thermal denaturation was followed by monitoring mean residue ellipticities at 222 nm (far-UV) using a Jobin-Yvon CD6 dichrograph interfaced with a Haake water bath. The signal was acquired with a 0.02 cm pathlength cell and a protein concentration of 30 μM with a sampling period of 60 s and an integration time of 1 s. The results were then averaged. The heating rate was 0.8 °C/min with a stabilization delay of 3 min before each recording.

Data Analysis—The measured fluorescence intensities and the mean residue ellipticity were analyzed in terms of a two-state transition to obtain the fraction of unfolded protein and free energy of folding as a function of denaturant. Non-linear least square fittings of the equilibrium transitions were achieved using the following equation,

$$S = S_n + nC + \frac{(S_u - S_n + (u - n)C)K}{1 + K} \qquad \text{(Eq. 1)}$$

where S is the signal (CD or fluorescence) measured, n and u the slopes of the native and unfolded base lines, S_u and S_n the specific signals of the native and unfolded protein extrapolated to zero denaturant concentration, and K the apparent equilibrium constant of unfolding at a concentration C of denaturant. The free energy of unfolding ΔG^0 at zero denaturant concentration is given by,

$$K = e\,\frac{(-\Delta G + mC)}{RTe} \qquad \text{(Eq. 2)}$$

where m is a constant characteristic of the protein and of the denaturant.

Stopped-flow Measurements—The measurements of $HasA_{SM}$ refolding kinetics were carried out at 22 °C with a SFM300 mixing device from Bio-logic (Pont de Claix, France). The mixing device, equipped with a F15 (1.5 × 1.5-mm cross-section) fluorescence cell, was combined with the optical bench and detection module from Bio-logic. The excitation wavelength was 295 nm, and the emitted light above 320 or 350 nm was detected through a high pass filter. The kinetics were recorded by means of the Bio-Kine software package from Bio-logic. For refolding experiments, 10 or 20 μl of denatured $HasA_{SM}$ (in 20 mM sodium phosphate, pH 7, and 5.5 M GdnHCl) were mixed with 390 or 380 μl of

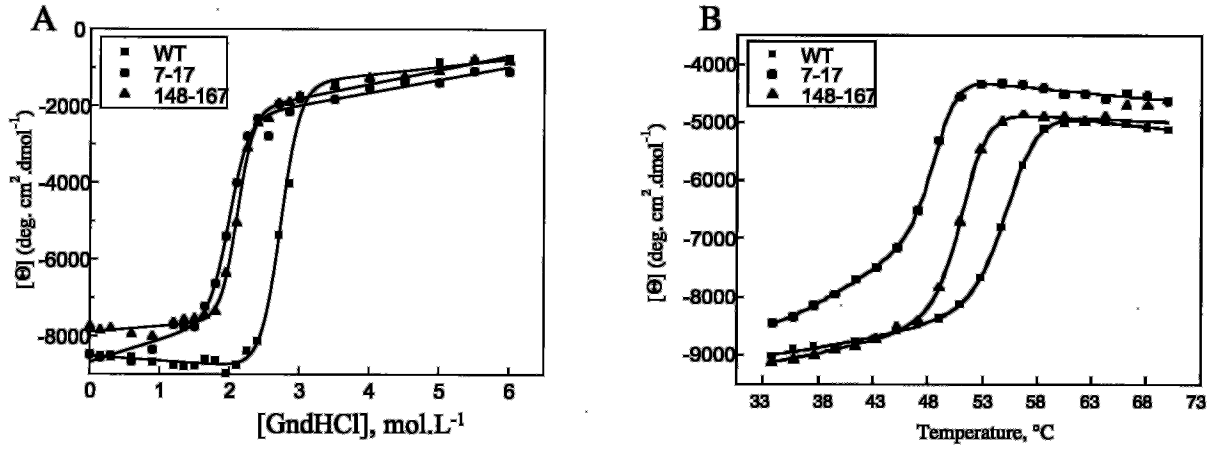

FIG. 1. **Guanidine HCl and thermal denaturation of WT and mutants $HasA_{SM}$.** *A*, GdnHCl denaturation; *B*, thermal denaturation. Denaturation was monitored by measurement of mean residue ellipticity at 222 nm. *Solid lines* are drawn according to the non-linear least square fittings of the equilibrium transitions using equations described under "Experimental Procedures." CD spectra were acquired in 20 mM sodium phosphate, pH 7.0, and at 25 °C for the chemical denaturation.

buffer (20 mM sodium phosphate, pH 7). The duration of the injections was 30 ms yielding a 4-ms dead time. Refolding kinetics were performed at various protein concentrations. For SecB-dependent refolding, SecB was added to the refolding buffer (from 7.5×10^{-3} μM to 1.5 μM SecB tetramer) with a final concentration of $HasA_{SM}$ of 0.375 and 0.75 μM. At either SecB concentration, kinetic traces were fitted using a multiexponential decay,

$$I = \sum_i A_i e^{-k_i' t} + A_\infty \qquad \text{(Eq. 3)}$$

where A_i is the amplitude of each phase, k_i its rate constant, and A_∞ is the plateau value.

RESULTS

Apo-$HasA_{SM}$ Unfolding and Refolding in Vitro $HasA_{SM}$ Refolds Spontaneously with Fast Kinetics—$HasA_{SM}$ is a 188-amino acid monomeric protein with a unique domain of α/β-fold (31). Fig. 1, *A* and *B*, show the chemical (Fig. 1*A*, *left*) and thermal (Fig. 1*B*, *right*) denaturations of WT $HasA_{SM}$ and of two mutants (see below for the description of the mutants), followed by monitoring the disappearance of the secondary structures using far-UV CD. During chemical denaturation of WT HasA, an increase in the fluorescence of the unique tryptophan was observed together with a shift in the maximum fluorescence emission wavelength (from 322 to 353 nm) (data not shown). Both fluorescence and far-UV CD (Fig. 1*A*) gave superimposable equilibrium denaturation curves using GdnHCl as denaturant. The data could be satisfactorily fitted to a two-state model $F \leftrightarrow U$ for unfolding. The GdnHCl concentration of half unfolding is given by $C_m = \Delta G/m$ and $C_m = 2.7 \pm 0.2$ M. The value obtained for the free energy of denaturation ΔG is 11.5 ± 4.7 kcal·mol^{-1}. As seen in thermal denaturation curve obtained for $HasA_{SM}$ using far-UV CD (Fig. 1*B*), the midpoint of the thermal transition T_m at 59.5 ± 0.5 °C is similar to the value reported by differential scanning calorimetry microcalorimetry.[2] Because this thermal transition of $HasA_{SM}$ is not reversible regardless of the heating rate chosen between 20 and 60 °C/h, we could not extract the thermodynamic parameters from the thermal denaturation data.

The refolding kinetics of WT Has_{SM} were also monitored by the fluorescence changes of its single tryptophan residue detected by a stopped-flow spectrophotometer (Fig. 2*A*, *trace a*). $HasA_{SM}$ is largely unfolded in 5.5 M GdnHCl and reversibly refolded upon dilution of the chaotropic agent leading to a large decrease of fluorescence. Upon dilution of apo-$HasA_{SM}$ from 5.5 M GdnHCl to 0.14 and 0.28 M GdnHCl, about 50% of the fluorescence intensity decreased within the dead time; nevertheless, this signal decrease is not due to a burst phase (phase faster than 4 ms) but rather to a dilution effect of GdnHCl. Indeed, extrapolation of fluorescence at 0.14 M GdnHCl from the curve obtained between 3.0 and 5.5 M GdnHCl gives the same intensity as this from the first fluorescence measurement in the denaturation kinetics (not shown). The time course of refolding as followed by Trp fluorescence, was fitted to a double exponential decay. The first phase (45 s^{-1}) corresponds to 92% of the relative amplitude, and the second (1.8 s^{-1}) accounts for the remaining 8% (see Fig. 3). These rate constants and amplitudes are only slightly temperature-dependent between 4 and 22 °C (data not shown).

SecB Slows Down in Vitro $HasA_{SM}$ Refolding—We have previously shown that $HasA_{SM}$ secretion is SecB-dependent in the original host and in the reconstituted system in *E. coli in vivo* (22, 23). This prompted us to study the *in vitro* interaction of SecB with $HasA_{SM}$. We could first show that no stable complexes exist between SecB and folded apo-$HasA_{SM}$ detected either by coimmunoprecipitation or by gel electrophoresis under non-denaturing conditions (data not shown). Apo-$HasA_{SM}$ refolding was also studied in the presence of various amounts of SecB in the renaturation buffer at 22 °C (Figs. 2*B* and 3). We used a high pass filter to collect emitted light above 350 nm to minimize the fluorescence contribution of SecB, which displays a maximum fluorescence emission around 320 nm in 0.14 M GdnHCl. Analysis of the refolding kinetics showed that SecB affects $HasA_{SM}$ folding (Fig. 2*B*, *traces a–e*). It is clear that SecB slows down HasA folding. This is a direct evidence for interaction, despite the very fast $HasA_{SM}$ folding kinetics. The folding of $HasA_{SM}$ is strongly retarded when more SecB is added to the refolding buffer (Fig. 2*B*, *traces a–e*). The $HasA_{SM}$-SecB interaction takes place very early, before or during the fast $HasA_{SM}$ folding phase (45 s^{-1}). Analysis of both amplitude and rate constant of the different phases observed in the presence of increasing amounts of SecB (Fig. 3) show the progressive appearance of a slow folding phase not observed in the absence of SecB. The amplitude of the major fast folding phase progressively decreases with higher concentrations of SecB, although the rate constant does not change at around 50 s^{-1}. A slower phase progressively appears with an apparent rate constant of 0.013 s^{-1}, at a 2:1 ratio of SecB tetramer to HasA; there is only a slight decrease of the rate constant with higher SecB concentrations. At the same time, the intermediate phase of 1.8 s^{-1} stays at the same small amplitude with a substoichiometric

[2] A. Lecroisey, personal communication.

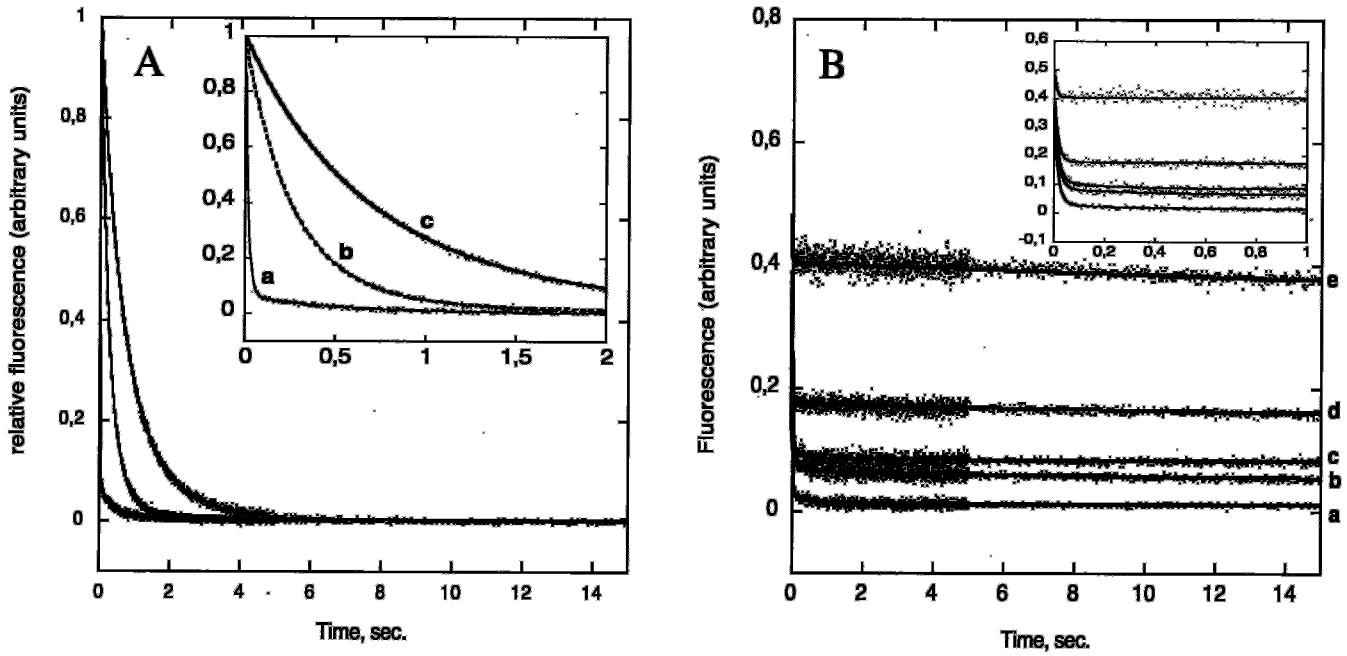

FIG. 2. **Refolding kinetics of WT and $HasA_{SM}$ mutants in the absence of SecB (*A*) and of WT $HasA_{SM}$ in the presence of SecB (*B*) at 22 °C measured by stopped-flow fluorescence.** *A*, the *solid lines* show the fits of the averaged kinetic traces to a bi-exponential decay. The *inset* shows the first 2 s: *trace a*, HasA; *trace b*, HasA148–167; *trace c*, HasA7–17. *B*, for SecB-dependent refolding, SecB was added to the refolding buffer: ratio of SecB tetramers/$HasA_{SM}$ of 0/0 (*trace a*), 1/50 (*trace b*), 1/25 (*trace c*), 1/5 (*trace d*), and 1/1 (*trace e*). The *solid lines* show the fits of the averaged kinetic traces to a tri-exponential decay. The *inset* shows the first second.

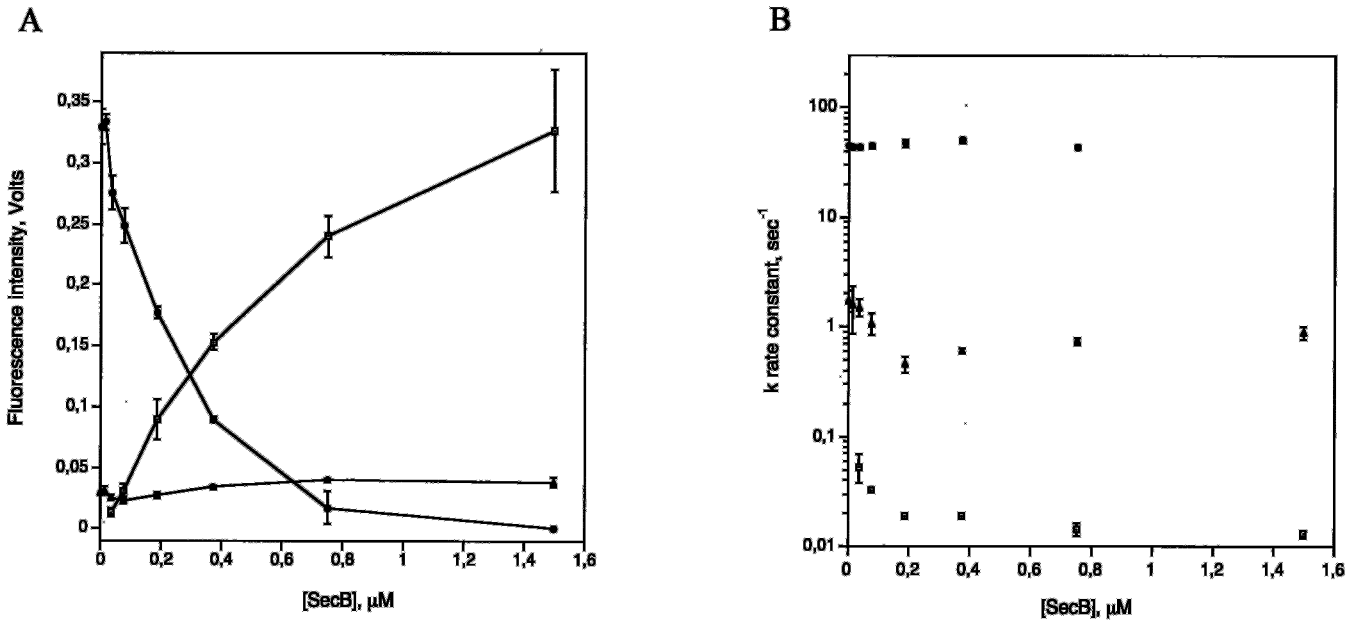

FIG. 3. **Phases of refolding of WT $HasA_{SM}$ in presence of increasing concentrations of SecB tetramer.** *A*, amplitude of the three refolding phases: a1 (●), a2 △); a3 (⊡). *B*, rate constants of the three refolding phases: k1 (●), k2 △; k3 (⊡). Stopped-flow fluorescence was measured at 22 °C with a final concentration of $HasA_{SM}$ at 0.75 μM in 20 mM sodium phosphate, pH 7.0. Each data point corresponds to the average of four to five independent kinetic series, each including nine successive individual traces that were averaged. The *error bars* represent the standard deviations. Each experiment was performed twice.

amount of SecB. Calculation of the stoichiometry of bound $HasA_{SM}$ to SecB, as extrapolated from the fluorescence data, indicated that this might vary from two $HasA_{SM}$ molecules bound per SecB tetramer at low SecB concentration to one $HasA_{SM}$ molecule bound per SecB tetramer at higher SecB concentration. As found for barnase in the presence of GroEl or SecB, addition of more SecB up to a 4:1 SecB:$HasA_{SM}$ ratio never blocked the folding of $HasA_{SM}$. Altogether our experiments indicate that $HasA_{SM}$ binds SecB tetramer with a 1:1 stoichiometry, and this considerably slows down the folding of $HasA_{SM}$, ~3200-fold. The very fast formation of $HasA_{SM}$·SecB complex suggests that the chaperone binds unfolded $HasA_{SM}$ or a very early folding intermediate. These experiments suggested that a function of SecB in HasA secretion would be antifolding and that slowly folding variants of HasA might be secreted independently of SecB.

N-terminal-C-terminal Interactions in $HasA_{SM}$ Affect Folding Rate but Not SecB Binding—We have proposed in previous studies that both the N- and C-terminal parts of $HasA_{SM}$ might be involved in the $HasA_{SM}$ secretion process (28, 29). Exami-

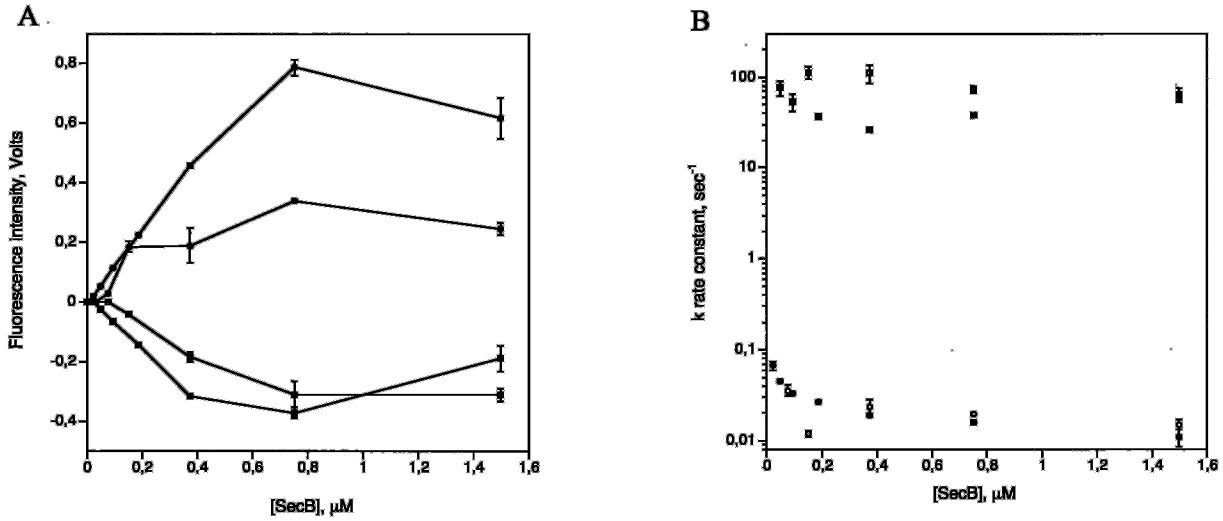

FIG. 4. **Phases of refolding of 7–17 and 148–167 mutants in presence of increasing concentrations of SecB tetramer.** *A*, amplitudes of the slow and fast refolding phases: 7–17 slow phase (●), 148–167 slow phase (○), 7–17 fast phase (■), 148–167 fast phase (□). *B*, rate constants of the slow and fast refolding phases: 7–17 slow phase (●), 148–167 slow phase (○), 7–17 fast phase (■), 148–167 fast phase (□). Stopped-flow fluorescence was measured at 22 °C with a final concentration of $HasA_{SM}$ at 0.75 μM in 20 mM sodium phosphate, pH 7.0. Each data point corresponds to the average of four independent kinetic series, each including nine successive individual traces. The *error bars* represent the S.D. values. Each experiment was performed twice.

nation of $HasA_{SM}$ x-ray structure indicates that there are two pairs of residues making side chain/side chain hydrogen bonds between these two extremities: Tyr^{7}/Asp^{167} and His^{17}/Glu^{148} (31). Based on the fact that the N- and C-terminal parts of $HasA_{SM}$ are involved in the secretion process and that theses extremities are in close contact in the native conformation, we postulated that mutations of those pairs of residues, by disrupting the hydrogen bonds, might affect folding rate and hence the SecB dependence of secretion. To this end these residues were individually changed for alanine, disrupting one hydrogen bond for each mutant protein. All those single residue mutants display reduced dependence upon SecB for secretion (data not shown). Two double mutants were thus constructed, Y7A,H17A and E148A,D167A, to disrupt both hydrogen bonds by mutating two residues either in the N terminus or the C terminus (see the figure provided in the Supplementary Material).

The refolding kinetics of $HasA_{SM}$7–17 and $HasA_{SM}$148–167 were studied using the same procedure as that for wild-type $HasA_{SM}$. Refolding of both mutants showed refolding kinetics much slower than that of wild-type (Fig. 2*A*, *traces b* and *c* as compared with *a*). Two distinct phases were detected for each mutant with no significant burst amplitude (Fig. 2). Fitting of the data showed that the 7–17 mutant displays one rate constant of 2.1 s^{-1} with relative amplitude of 68% and one rate constant of 0.9 s^{-1} and its relative amplitude of 30%. The two phases detected for 148–167 have rate constants of 3.9 and 1 s^{-1} with respective relative amplitudes of 83 and 17%. These data do not allow us to conclude that mutants and wild-type $HasA_{SM}$ follow the same folding pathway or different folding pathways.

In the presence of SecB, both mutants displayed essentially similar behavior and, as for WT HasA, their refolding kinetics is slowed down (not shown), indicative of an interaction with SecB. However, fitting of the data required four exponentials, instead of three for the WT. The Fig. 4 shows the analysis of the fluorescence data for the mutants in a similar way as that done for WT HasA. The amplitudes of the two refolding phases of HasA mutants, observed in the absence of SecB decreased, while two (negative) amplitudes appeared and increased with the concentration of SecB (not represented on Fig. 4). The corresponding phases could correspond to isomerizations of the HasA·SecB complex. Additionally, a fast phase, characterized by an increase of fluorescence emission, is observed upon SecB addition. At a 2:1 ratio of SecB tetramer to HasA, the apparent rate constants of this fast phase are 64.4 s^{-1} for 7–17 and 61.8 s^{-1} for 148–167, respectively. This fast initial phase could correspond to the binding of HasA to SecB (see Fig. 4). Furthermore a slow phase of positive amplitude appeared with the same apparent rate constant as that of the wild-type: at a 2:1 ratio of SecB tetramer to HasA, rate constants of this slow phase were of 0.011 s^{-1} for 7–17 and 0.015 s^{-1} for 148–167, respectively (see Fig. 4). This phase can correspond, as for WT HasA, to the slow dissociation of HasA, partially or totally folded, from the HasA·SecB complex. As also has been seen with the wild type HasA, folding is never blocked, only strongly retarded, whatever the concentration of chaperone. Finally, SecB is able to interact with the mutants that are indistinguishable from the wild-type with regards to this phenomenon, at our level of analysis.

Interactions between the N and C Terminus of $HasA_{SM}$ Affect SecB Dependence for Secretion but Not $HasA_{SM}$ Function— These two double mutants were tested for their secretion and found to be mostly SecB-independent (Fig. 5). Furthermore, the biological activities of the two mutants were indistinguishable from the wild-type (data not shown). Their far-UV and near-UV CD spectra were also identical to that of the wild-type (Fig. 6), indicating that mutant proteins essentially maintain their secondary and tertiary structures. Their behavior in terms of secretion strongly supported our model as it appears that slowing down their folding kinetics correlates with their reduced SecB dependence in terms of secretion.

CD (Fig. 1) and fluorescence (not shown) spectra were recorded at several GdnHCl concentrations for the mutants. Like the wild-type protein, the UV CD and fluorescence of 7–17 and 148–167 mutants showed a clear cooperative GdnHCl-induced transition (Fig. 1*A*). It was found that half-denaturation occurred at lower GdnHCl concentration than for wild-type, consistent with a reduced stability of the mutants. A two-state analysis of the data gave midpoints (C_m) of 1.99 ± 0.2 M for protein 7–17 and 2.1 ± 0.2 M for protein 148–167. The free energies of denaturation (ΔG) is 8.4 ± 1.9 kcal·mol^{-1} for 7–17 and and 10.6 ± 2.8 kcal·mol^{-1} for 148–167. Differences of ΔG between mutant and wild-type $HasA_{SM}$ are compatible with

the loss of two hydrogen bonds (about 4 kcal·mol^{-1}) as a result of the mutations. Although the $HasA_{SM}$ mutants are destabilized with respect to the wild-type protein, their fractions of unfolded molecules at 0 M GdnHCl extracted from the free energy of denaturation remain very low: 7.8×10^{-7} for the 7–17 mutant and 1.8×10^{-8} for the 148–167 mutant *versus* 3.9×10^{-9} for the wild-type protein. Thermal unfolding also indicated a lower stability of both mutant proteins (Fig. 1*B*). The midpoint values of the thermal transition T_m are 52.6 ± 0.5 °C for 7–17 and 55.0 ± 0.5 °C for 148–167.

As a control we used another double mutant of HasA, H32A,Y75A, affecting heme binding (32). This mutant had a somewhat reduced stability (half-denaturation at 2.2 ± 0.2 M), refolded with the same kinetics as that of the wild-type protein, and was SecB-dependent for its secretion at the same extent as wild-type protein (data not shown).

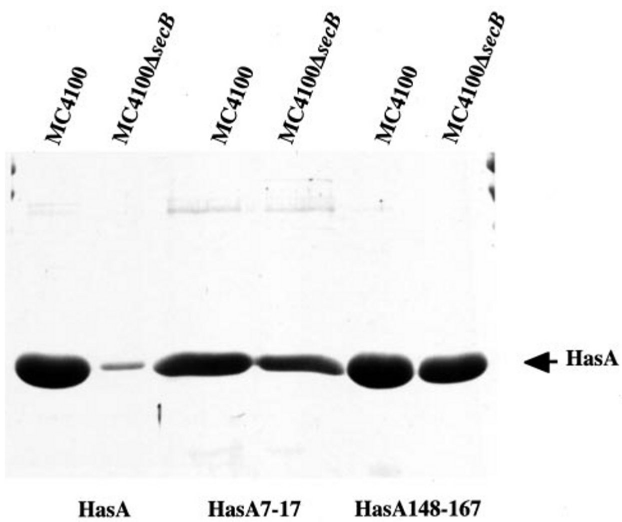

FIG. 5. **Secretion of wild-type and mutant HasA in SecB-plus and SecB-minus backgrounds.** SDS-PAGE of supernatants from strains MC4100 or MC4100Δ*secB* containing Has secretion functions from pSYC150 and wild-type or mutant HasA on a compatible plasmid are shown. The amounts correspond to 0.5 $OD_{600\ nm}$ except for mutant HasA 7–17, where 2 $OD_{600\ nm}$ were loaded.

DISCUSSION

Here we have studied $HasA_{SM}$ folding and its interaction with SecB *in vitro* together with the effect of mutations disrupting hydrogen bonds between the C and N terminus of $HasA_{SM}$ on its folding and their secretion dependence upon SecB. $HasA_{SM}$ folding is simple with no burst-phase intermediate and with a fast and major folding phase, making it an attractive model to study interactions with SecB. This is the first time a natural SecB-dependent substrate that is not a Sec substrate has been studied in interaction with SecB *in vitro*.

The interaction between $HasA_{SM}$ and SecB differs in several characteristics of the interaction of SecB with Sec substrates. Since $HasA_{SM}$ and the mutants do not contain any arginine or lysine and are mostly negatively charged, the basis of interaction between $HasA_{SM}$ and SecB cannot rely on electrostatic interaction between residues but through hydrophobic interactions (33, 34). Since $HasA_{SM}$ is a natural substrate of SecB, the absence of positive charge in $HasA_{SM}$ proves that positive charges are not a prerequisite for interaction with SecB. As seen with other substrates, SecB slows down HasA folding by more than three orders of magnitude. However, in contrast to the MBP or galactose-binding protein refolding, which is totally blocked at high SecB concentrations, which allows the isolation of permanent stable complexes (12, 18), this does not appear to be the case for $HasA_{SM}$. Instead, there appears to be a slow folding phase of 0.014 s^{-1} whose apparent rate constant does not significantly change with varying SecB amounts.

$$ {}_{U}HasA_{SM} + SecB \leftrightharpoons {}_{U}HasA_{SM} \cdot SecB \rightharpoonup {}_{N}HasA_{SM} \cdot SecB \rightharpoonup {}_{N}HasA_{SM}\ SecB $$
$$ \downarrow $$
$$ {}_{U}HasA_{SM} $$

REACTION 1

This is reminiscent of the behavior of barnase (a synthetic SecB substrate) in the presence of SecB, which has been interpreted as at least partial refolding when bound to this chaperone (20). This is in contrast to the model of kinetic partitioning like for MBP in which the unfolded protein is bound to SecB, released, and folded only when free in solution. It is likely what happens with barnase occurs with $HasA_{SM}$.

The major folding phase of $HasA_{SM}$ has a rate constant inferior to 45 s^{-1}, which is much faster than the rate constants observed for characterized substrates of the Sec system. Fur-

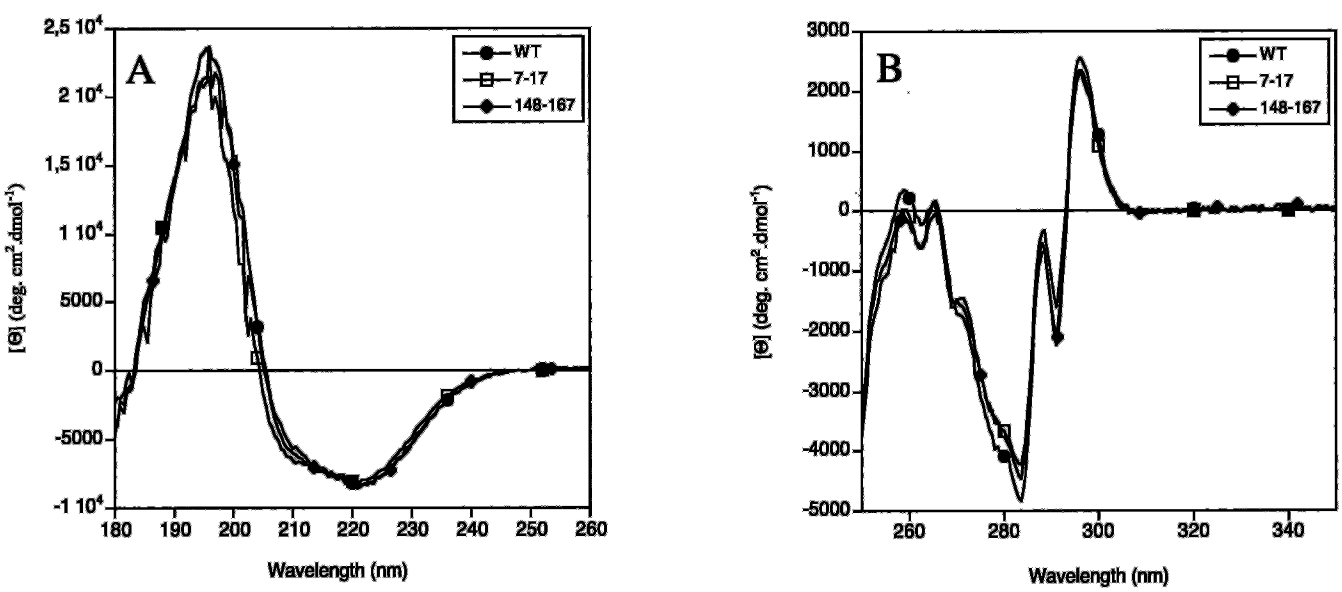

FIG. 6. **Secondary and tertiary structures of wild-type and $HasA_{SM}$ mutants mapped by far- and near-UV CD experiments.** *A*, far-UV spectra; *B*, near-UV spectra. CD was acquired at 30 μM of protein concentration in 20 mM sodium phosphate, pH 7.0, 25 °C.

thermore, in the case of Sec substrates, the presence of the signal sequence slows down folding. This has been proposed as the basis of the *in vivo* selectivity of SecB for its substrates (10, 16); this clearly does not apply to the case of $HasA_{SM}$. SecB binds to $HasA_{SM}$ in millisecond time scale. At 1:1 $HasA_{SM}$:SecB stoichiometry, we estimated the second-order binding rate constant at 3×10^9 M^{-1} s^{-1}, suggesting that the rate of $HasA_{SM}$ association to SecB is diffusion-limited (21). So, a slow folding kinetics is not a prerequisite for *in vivo* implication of SecB in this case. It is very likely that this explains that secretion competence of $HasA_{SM}$ cannot be observed for a long period of time, since uncoupling of $HasA_{SM}$ synthesis from its secretion apparatus leads to no secretion even when SecB is overexpressed (29). Moreover this is consistent with the observed absence of blockage of folding of $HasA_{SM}$ by SecB.

In the Sec system, SecB fulfills two separate functions of slowing down precursor folding and of targeting to SecA, the ATPase of the Sec system (35). In the ABC system of $HasA_{SM}$ secretion, the precise functions of SecB are not known. Here, we have shown that SecB is able to strongly slow down the folding of wild-type $HasA_{SM}$ and that the secretion of the slower folding variants of $HasA_{SM}$ is much less SecB-dependent than the secretion of wild-type $HasA_{SM}$. Given the fact that folded $HasA_{SM}$ is no longer secretion competent, it, thus, seems that the main role of SecB in the ABC system is slowing down $HasA_{SM}$ folding. The behavior of the two mutants we have constructed also supports the importance of slowing down of folding function of SecB in this system. Although it is difficult to extrapolate from the *in vitro* folding kinetics to *in vivo*, it is clear that both mutants fold more slowly than wild-type $HasA_{SM}$. We conclude that interactions between the N terminus and the C terminus of the protein are at least involved in the rapid folding kinetics of $HasA_{SM}$. The mutants were secreted to a significant extent in the absence of SecB, they were fully functional, and they were indistinguishable from wild-type in terms of global fold. Although both mutants display a reduced stability as observed with the thermal and chemical denaturations, the very low fraction of unfolded proteins in "native" conditions seems insufficient to explain their efficient secretion in the absence of SecB, especially, in light of the fact that HasA32–75, which has the same reduced stability, is as SecB-dependent as the wild-type. SecB interacts with wild-type and mutant $HasA_{SM}$ so as to slow down their folding. Although able to interact with $HasA_{SM}$ mutants, SecB has little effect on their secretion; this is also what was observed for the SecB independent mutant of MBP. In the Sec system, a cascade of increasing binding affinities allows the transfer of the precursor from SecB to SecA and to the translocon (35). This might not occur in the case of $HasA_{SM}$ if folding still occurs on SecB; efficient secretion would result from competition between folding and secretion. In the Sec system SecB has an essential targeting function to the SecA ATPase and an antifolding function. In the HasA ABC secretion system, SecB has an antifolding function. We have previously shown that the N-terminal part of HasA is involved in efficient secretion and in an early interaction with the transporter. It remains to be determined whether SecB plays a role in this interaction.

We had proposed that both the C terminus of $HasA_{SM}$ bearing the secretion signal and the N terminus part of $HasA_{SM}$ via a SecB-dependent recognition of the transporter were involved in efficient $HasA_{SM}$ secretion (28). The behavior of the mutants might give clues on how this could happen; one of the functions of SecB, upon binding to $HasA_{SM}$, would keep both ends of $HasA_{SM}$ freely available to the transporter. If one assumes that the SecB binding sites defined by the peptide library technique are relevant to the *in vivo* situation, there appears to be only one such site in $HasA_{SM}$ fulfilling the criteria defined (9). This site is at the N terminus of $HasA_{SM}$ between residues 18–28, YLGQWASTFG, with three aromatic residues and no negative charge. The N-terminal position of the putative binding site of SecB and the very fast folding *in vitro* of $HasA_{SM}$ suggest that the chaperone would bind the nascent chain of $HasA_{SM}$. This is in agreement with our model of secretion in which $HasA_{SM}$ is targeted in a cotranslational fashion to the ABC transporter (29).

Acknowledgments—We thank C. Wandersman for helpful discussions and critical reading of the manuscript and J. M. Betton for gift of the SecB overproducing plasmid.

REFERENCES

1. Kumamoto, C. A., and Beckwith, J. (1983) *J. Bacteriol.* **154,** 253–260
2. Collier, D. N., Bankaitis, V. A., Weiss, J. B., and Bassford, P. J., Jr. (1988) *Cell* **53,** 273–283
3. Weiss, J. B., Ray, P. H., and Bassford, P. J., Jr. (1988) *Proc. Natl. Acad. Sci. U. S. A.* **85,** 8978–8982
4. Hartl, F. U., Lecker, S., Schiebel, E., Hendrick, J. P., and Wickner, W. (1990) *Cell* **63,** 269–279
5. Driessen, A. J. (2001) *Trends Microbiol.* **9,** 193–196
6. Kumamoto, C. A., and Francetic, O. (1993) *J. Bacteriol.* **175,** 2184–2188
7. Collier, D. N. (1993) *Adv. Protein Chem.* **44,** 151–193
8. Xu, Z., Knafels, J. D., and Yoshino, K. (2000) *Nat. Struct. Biol.* **7,** 1172–1177
9. Knoblauch, N. T., Rudiger, S., Schonfeld, H. J., Driessen, A. J., Schneider-Mergener, J., and Bukau, B. (1999) *J. Biol. Chem.* **274,** 34219–34225
10. Hardy, S. J., and Randall, L. L. (1991) *Science* **251,** 439–443
11. Khisty, V. J., and Randall, L. L. (1995) *J. Bacteriol.* **177,** 3277–3282
12. Diamond, D. L., and Randall, L. L. (1997) *J. Biol. Chem.* **272,** 28994–28998
13. Topping, T. B., and Randall, L. L. (1997) *J. Biol. Chem.* **272,** 19314–19318
14. Collier, D. N., and Bassford, P. J., Jr. (1989) *J. Bacteriol.* **171,** 4640–4647
15. Altman, E., Bankaitis, V. A., and Emr, S. D. (1990) *J. Biol. Chem.* **265,** 18148–18153
16. Liu, G., Topping, T. B., and Randall, L. L. (1989) *Proc. Natl. Acad. Sci. U. S. A.* **86,** 9213–9217
17. Topping, T. B., and Randall, L. L. (1994) *Protein Sci.* **3,** 730–736
18. Khisty, V. J., Munske, G. R., and Randall, L. L. (1995) *J. Biol. Chem.* **270,** 25920–25927
19. Smith, V. F., Hardy, S. J., and Randall, L. L. (1997) *Protein Sci.* **6,** 1746–1755
20. Stenberg, G., and Fersht, A. R. (1997) *J. Mol. Biol.* **274,** 268–275
21. Fekkes, P., den Blaauwen, T., and Driessen, A. J. (1995) *Biochemistry* **34,** 10078–10085
22. Delepelaire, P., and Wandersman, C. (1998) *EMBO J.* **17,** 936–944
23. Sapriel, G., Wandersman, C., and Delepelaire, P. (2003) *J. Bacteriol.* **185,** 80–88
24. Létoffé, S., Ghigo, J. M., and Wandersman, C. (1994) *J. Bacteriol.* **176,** 5372–5377
25. Létoffé, S., Redeker, V., and Wandersman, C. (1998) *Mol. Microbiol.* **28,** 1223–1234
26. Rossi, M. S., Fetherston, J. D., Létoffé, S., Carniel, E., Perry, R. D., and Ghigo, J. M. (2001) *Infect. Immun.* **69,** 6707–6717
27. Ghigo, J.-M., Létoffé, S., and Wandersman, C. (1997) *J. Bacteriol.* **179,** 3572–3579
28. Sapriel, G., Wandersman, C., and Delepelaire, P. (2002) *J. Biol. Chem.* **277,** 6726–6732
29. Debarbieux, L., and Wandersman, C. (2001) *EMBO J.* **20,** 4657–4663
30. Izadi, N., Henry, Y., Haladjian, J., Goldberg, M. E., Wandersman, C., Delepierre, M., and Lecroisey, A. (1997) *Biochemistry* **36,** 7050–7057
31. Arnoux, P., Haser, R., Izadi, N., Lecroisey, A. D., M., Wandersman, C., and Czjzek, M. (1999) *Nat. Struct. Biol.* **6,** 516–520
32. Létoffé, S., Deniau, C., Wolff, N., Dassa, E., Delepelaire, P., Lecroisey, A., and Wandersman, C. (2001) *Mol. Microbiol.* **41,** 439–450
33. Randall, L. L. (1992) *Science* **257,** 241–245
34. Hardy, S. J., and Randall, L. L. (1993) *Philos. Trans. R. Soc. Lond. Ser. B Biol. Sci.* **339,** 343–354
35. Fekkes, P., and Driessen, A. J. (1999) *Microbiol. Mol. Biol. Rev.* **63,** 161–173